Evidence for Supersonic Turbulence in the Upper Atmosphere of Jupiter

Claude Emerich,* Lotfi Ben Jaffel, John T. Clarke, Renée Prangé, G. Randall Gladstone, Joel Sommeria, Gilda Ballester

Spectra of the hydrogen Lyman α (Ly-α) emission line profiles of the jovian dayglow, obtained by the Goddard High Resolution Spectrograph on the Hubble Space Telescope, appear complex and variable on time scales of a few minutes. Dramatic changes occur in the Ly-α bulge region at low latitudes, where the line profiles exhibit structures that correspond to supersonic velocities of the order of several to tens of kilometers per second. This behavior, unexpected in a planetary atmosphere, is evidence for the particularly stormy jovian upper atmosphere, not unlike a star's atmosphere.

The upper atmospheric thermal excess observed for the outer giant planets in the Voyager missions (*1, 2*) is one of the outstanding dilemmas in the study of their atmospheres. Their exospheric temperatures are greater than the temperatures expected from solar heating of the upper atmosphere alone (*3*). Another puzzling phenomenon, the H Ly-α bulge, consists of a region of enhanced H Ly-α brightness along the magnetic drift equator in Jupiter's atmosphere, with a maximum at a magnetic longitude of about 100° (System III) (*1, 2, 4–6*). An important clue to the nature of this phenomenon is the fact that no corresponding enhancement was observed in the H_2 Lyman and Werner band emissions (*7*). More recently, high-resolution International Ultraviolet Explorer (IUE) measurements (~0.14 Å) of the H Ly-α line profiles in the jovian equatorial bulge region (*6*) revealed a broadening of the line core. By contrast, the lines from mid-latitudes and in the antibulge region showed less brightening and broadening, unambiguously demonstrating that the Ly-α bulge is associated with an H line broadening rather than with an enhancement of the brightness near the Ly-α line center (*8*). This result ruled out the excitation of the bulge by electron impact on ambient H atoms, suggested as being part of the electroglow process (*9, 10*).

Two remaining possible mechanisms to explain the bulge are (i) it is a superthermal population of H atoms produced by collisional processes analogous to the equatorial anomaly or tropical arcs on Earth (*8*) or (ii) it is an atmospheric turbulence in the upper thermosphere of Jupiter, producing velocities from 5 to 10 km s^{-1}, that enhances the width of the H Ly-α resonance cross section (*9*). At this time, the first mechanism has not been used for quantitative modeling of the Ly-α line profile. The second mechanism has been modeled (*9*) in terms of a nonthermal velocity field confined to an active layer located in the upper atmosphere of Jupiter at the ~1-nbar pressure level and representing less than 1% of the total atmospheric content of H. Although other processes cannot be rejected at the moment, it was recently suggested (*11*) that such turbulence could be produced by the collision in the bulge area of two supersonic jets generated by the energy deposited in the auroral regions (≃10^{14} W). These jets, supposedly created in the region of the northern and southern auroral ovals, could collide in the bulge region, inducing turbulent effects and consequently a global enhancement of the temperature (*11*). However, no direct evidence of jets or turbulence has been observed. Because the Ly-α line emission is a good tracer of the upper atmospheric structure, the atmosphere variability should be studied through direct detection of variable and multicomponent line profiles (*12, 13*). Therefore, to better describe and understand the upper jovian atmosphere, we report here observations of the profiles of the H Ly-α line emission of Jupiter at the low-latitude regions of the H Ly-α bulge.

These spectra were measured with the Goddard High Resolution Spectrograph (GHRS) Echelle-A grating and the 1.7–arc sec square aperture [large science aperture (LSA)], whose projection on Jupiter's disk covered a region of ≈8000 km by 8000 km at the equator. The pointing was done by direct offset from the Galilean satellite Io, with an estimated uncertainty of ~0.1 arc sec. Deviations from the standard Space Telescope Science Institute (STScI) reduction and calibration procedures have been made to suppress the light diffused from the neighboring orders of the echelle grating (*14*) and to correct for a faulty on-board Doppler compensation (*15*). Moreover, because the Hubble Space Telescope (HST) orbits within the atmosphere of Earth, the measured spectra are the sum of the atomic H Ly-α emissions of the jovian atmosphere and of the sky-background resulting from the geocorona and the interplanetary medium (IPM). We measured this sky-background contribution in a separate sequence, by pointing the aperture off Jupiter's disk by ~3 arc min. We then deduced the Ly-α emission of Jupiter by scaling and subtracting the sky-background from each measured spectrum (*16*) (Fig. 1).

Bulge Ly-α line profiles for two different longitudes (Fig. 2 and Table 1) (*17*) show

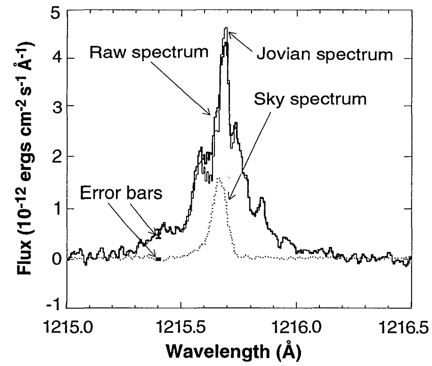

Fig. 1. Hydrogen Ly-α line profiles before and after correction for sky background (*16*). The upper and lower error bars represent the measurement uncertainties on, respectively, the jovian (raw and corrected) spectra and the sky-background spectrum.

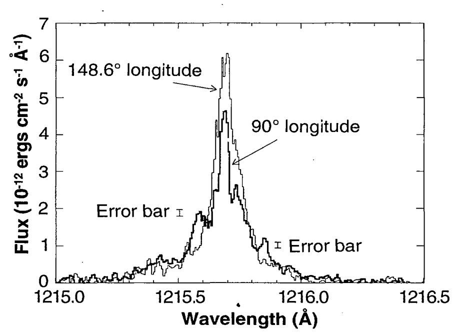

Fig. 2. Two corrected H Ly-α line profiles measured in the jovian bulge region. The exposures of about 16 min each were taken about 20 hours apart (Table 1). The mean uncertainties on both profiles are represented by the error bars. The most disturbed profile, obtained at 90° longitude, corresponds to the core of the bulge, which should be the most active region.

C. Emerich and R. Prangé, Institut d'Astrophysique Spatiale, CNRS, F-91405 Orsay, France, and Institut d'Astrophysique de Paris, CNRS, F-75014 Paris, France.
L. Ben Jaffel, Institut d'Astrophysique de Paris, CNRS, F-75014 Paris, France.
J. T. Clarke and G. Ballester, Space Physics Research Laboratory, University of Michigan, Ann Arbor, MI 48109–2143, USA.
G. R. Gladstone, Southwest Research Institute, San Antonio, TX 78238, USA.
J. Sommeria, Ecole Normale Supérieure de Lyon, Lyon, France.

*To whom correspondence should be addressed.

that (i) the profiles are disturbed with sharp spikes narrower than the ~0.07 Å of the LSA spectral line spread function (*18*) and (ii) the spectra vary on a time scale of the order of some minutes (Fig. 3, A through D). The unusual features apparent in the observed line profiles are distributed at Doppler shifts from the line center corresponding to supersonic velocities ranging from a few to a few tens of kilometers per second. These features can be attributed to the occurrence of H cells ≤1000 km by 8000 km in area (*19*), progressing randomly through the GHRS field of view at high velocities and varying on time scales of the order of a few minutes or less. Although radiative transfer and opacity effects may affect any interpretation of the observed features in terms of moving H cells, a crude estimate of their characteristics can be made by measuring the intensity of the features appearing above and below the time-averaged spectrum. From Figs. 2 and 3, we estimated that these H cells move at a mean velocity of ~5 km s^{-1} (with a standard deviation of ~40 km s^{-1}) and correspond to H column densities ≈ 5×10^{11} to 10×10^{11} cm^{-2}. If the emissions are entirely due to resonantly scattered sunlight, this also corresponds to a mean total number of H atoms per cell of ≈ 4×10^{28} to 8×10^{28}. If we assume a Gaussian velocity field, we can deduce that a population of fast atomic H should overcome the planet's gravity force and escape at a rate of ~10^{29} atoms per second over the extent of the bulge area (*20*). Such chaotic motions support a model of atmospheric supersonic turbulence in the region of the bulge (*9*).

A complete model of the line profile structure would require an accurate description of the turbulence and the solution of a complex stochastic radiative transfer equation (*21*). Moreover, the supersonic behavior of the velocity field introduces nonlinear effects that strengthen the atmosphere–radiation field coupling, making the simulation of the radiation field even more difficult. However, in an attempt to describe the problem, we have assumed a stationary microturbulent velocity field, which gives a more tractable radiative transfer equation. We solved the radiative transfer equation using the model parameters of the turbulent atmosphere that fit the IUE data (*9, 22*). For comparison, calculations were also carried out in the case of a static atmosphere. These calculated line profiles were compared to the averaged spectra measured in the bulge region (Fig. 4).

Although the integrated intensity can be reproduced with the IUE model parameters, none of the models can reproduce the line profiles of the present higher resolution GHRS observations, no matter what microturbulent velocities or total H column in a static atmosphere are assumed (*22*). This fact is consistent with the high-velocity dispersion derived from Fig. 3, which is the signature of a violent process that cannot be described in detail by any stationary or static microturbulent model (*23*).

More sophisticated modeling of the turbulence and the bulk motions observed in the upper layers of the jovian atmosphere is needed. This modeling should take into account the finite size of the moving cells and the time evolution of the process.

Table 1. GHRS observations of H Ly-α emissions from the jovian bulge emission.

Target	Date (julian date) (1994)	Time (universal time)	Exposure (s)	Longitude	I^* (kR)
Sky-background	9 May	16:05:17	734.4	Off disk	1.6
Bulge	27 May	18:30:53	979.2	90°	8.8
Bulge	28 May	15:26:29	979.2	148.6°	9.8

*Line-integrated intensities in kilorayleighs, after corrections and scaling.

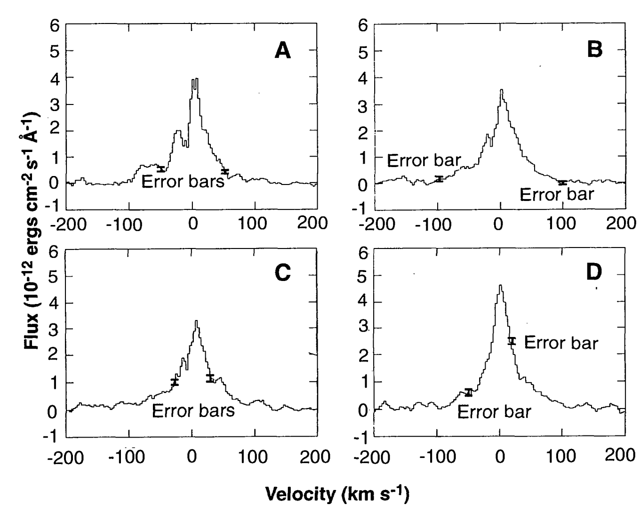

Fig. 3. Time evolution of the jovian line profiles in the core of the bulge region. Each of the four consecutive subspectra (**A** through **D**) represents 4 min of exposure time. The binning has been chosen to obtain the same signal-to-noise ratio as that in the preceding figures (*16*). The time measurement for (A) is given in Table 1. The average of the four subspectra corresponds to the line profile of the core of the bulge shown in Fig. 2 (bold solid line). To show the involved motions, we have converted the wavelength scale into Doppler velocities.

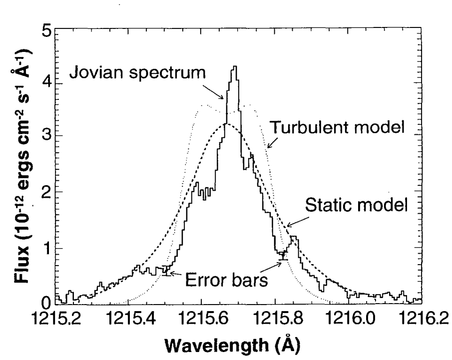

Fig. 4. Comparison of one measured HST bulge spectrum with line profiles calculated using model parameters deduced from IUE measurements (*22*). The microturbulent model has [H] = 3×10^{17} cm^{-2} and a turbulent velocity of 7 km s^{-1}. The static model corresponds to a temperature of 1100 K and to [H] = 5×10^{17} cm^{-2}. The discrepancies with the observations arise from the incompatibility between the assumed stationary models and a quickly evolving process.

REFERENCES AND NOTES

1. J. T. Clarke *et al.*, *Astrophys. J.* **240**, 696 (1980).
2. B. R. Sandel, A. L. Broadfoot, D. F. Strobel, *Geophys. Res. Lett.* **7**, 5 (1980).
3. S. K. Atreya *et al.*, *ibid.* **6**, 795 (1979).
4. A. J. Dessler, B. R. Sandel, S. K. Atreya, *Planet. Space Sci.* **29**, 215 (1981).
5. T. E. Skinner *et al.*, *J. Geophys. Res.* **93**, 29 (1988).
6. M. A. McGrath, *Geophys. Res. Lett.* **18**, 1931 (1991).
7. ______, G. E. Ballester, H. W. Moos, *J. Geophys. Res.* **95**, 365 (1990).
8. J. T. Clarke, G. R. Gladstone, L. Ben Jaffel, *Geophys. Res. Lett.* **18**, 1935 (1991).
9. L. Ben Jaffel *et al.*, *ibid.* **20**, 747 (1993).
10. D. E. Shemansky, *J. Geophys. Res.* **90**, 2673 (1985).
11. J. Sommeria, L. Ben Jaffel, R. Prangé, *Icarus* **119**, 2 (1995).
12. C. Magnan, *J. Quant. Spectrosc. Radiat. Transfer* **16**, 281 (1976).
13. M. L. Loucif and C. Magnan, *Astron. Astrophys.* **112**, 287 (1982).
14. The automatic procedure to subtract the interorder background between the echelle orders is not adapted for measurements of a diffuse emission that fills the aperture. Consequently, the spectra were reduced without interorder background subtraction, and we later subtracted a constant background determined from adjacent wavelengths.
15. The automatic on-board correction for the effects of the motion of HST had been calculated in the initial reduction on the basis of erroneous coordinates for the moving targets. Consequently, the correct com-

pensations were recalculated by the HST staff and then introduced into our data analysis of each individual spectrum. This procedure and the new Doppler corrections were validated by the spectrum obtained for the sky-background measurements: The central wavelength corresponding to the Ly-α resonance line was precisely located at its laboratory value of 1215.67 Å, within the experimental accuracy (about 0.008 Å) (Fig. 1).
16. The IPM and geocoronal H also contributed some extinction to the jovian signal before it was measured by HST. The jovian profile deduced from all of these corrections was almost equal to the raw measured profile (Fig. 1). This is so because of the opposite effects of a small background subtraction and of the geocoronal and IPM extinction. Finally, we improved the measured signal-to-noise ratio by binning the spectra by pairs of pixels (for exposures of 16 min) and by four pixels (for exposures of 4 min).
17. Each mean spectrum in Fig. 2 is the average of 16 elementary exposures of ≈1 min. Each subspectrum in Fig. 3 is the average of four of these elementary exposures.
18. The spectral line spread function is the wavelength width measured by the instrument when exposed to an extended monochromatic source illuminating the whole detector. If a quasi-monochromatic source illuminates only one of the eight diodes of the GHRS detector, the measured width may be as small as ~0.07 Å/8 ~ 0.009 Å.
19. One such cell within the GHRS Science slit corresponds to the projection on Jupiter's disk of one GHRS diode (in the dispersion axis) by eight diodes in the perpendicular axis.
20. The bulge area can be estimated from the Voyager Ly-α isophote maps given in (4). If R_J is the jovian radius, it amounts $\pi/4 \times \pi/10 \times R_J^2 \sim 3.6 \times 10^8$ km^2.
21. C. Magnan, *Astron. Astrophys.* **144**, 186 (1985).
22. The IUE data were fitted by a total H column density [H] ≈ 3×10^{17} to 4×10^{17} cm^{-2} [that is, three to four times the [H] derived from photochemistry models based on the Voyager Ultraviolet Spectrometer (UVS) occultation observations (9)] and velocities in the range 5 to 7 km s^{-1}. These effective velocities correspond to the active layer assumed to mimic the region where the bulge effect occurs. The integrated flux of the solar Ly-α line corresponding to the present observations was ≈2.6×10^{11} photons per square centimeter per second at 1 astronomical unit.
23. The fact that these models were able to roughly fit the profiles measured by IUE appears to be due to the much longer integration time of these observations, which averaged out the fine structure of any line profile (spectral or temporal) that the higher sensitivity of HST-GHRS is now able to detect almost instantaneously.
24. The work of C.E., L.B.J., and R.P. was supported by CNRS and the Institut National des Sciences de l'Univers (INSU). The work of J.C. and G.B. was supported under NASA grant STScI GO-5417.01-93A. The work of R.G. was supported under STScI grant GO-5417.02-93A. This work is based on observations with the NASA–European Space Agency HST, obtained at the STScI, which is operated by the Association of Universities for Research in Astronomy for NASA under contract NAS 5-26535.

17 April 1996; accepted 5 July 1996

Rapid Variations in Atmospheric Methane Concentration During the Past 110,000 Years

Edward J. Brook, Todd Sowers, Joe Orchardo

A methane record from the GISP2 ice core reveals that millennial-scale variations in atmospheric methane concentration characterized much of the past 110,00 years. As previously observed in a shorter record from central Greenland, abrupt concentration shifts of about 50 to 300 parts per billion by volume were coeval with most of the interstadial warming events (better known as Dansgaard-Oeschger events) recorded in the GISP2 ice core throughout the last glacial period. The magnitude of the rapid concentration shifts varied on a longer time scale in a manner consistent with variations in Northern Hemisphere summer insolation, which suggests that insolation may have modulated the effects of interstadial climate change on the terrestrial biosphere.

Atmospheric methane concentration variations recorded in ice cores have the potential to reveal past changes in terrestrial methane emissions, driven primarily by changes in temperature and precipitation, as well as changes in the primary methane sink, oxidation by tropospheric OH. Because the atmospheric mixing time is short relative to the methane lifetime, and because methane sources and sinks have a wide geographic distribution, methane concentration variations recorded in ice cores are believed to reflect large-scale and perhaps global changes in the methane budget. Comparison of ice core methane records with other proxy climate records that are believed to reflect more regional climate variability (such as dust or the isotopic composition of ice) can provide constraints on the global significance of the regional variations.

E. J. Brook and J. Orchardo, Graduate School of Oceanography, University of Rhode Island, Narragansett, RI 02882, USA.
T. Sowers, 447 Deike Building, Geosciences Department, Pennsylvania State University, University Park, PA 16802, USA.

A long record from the Vostok ice core (East Antarctica) (*1, 2*) showed that over the past 225,000 years, atmospheric methane concentrations ranged from glacial values of ~350 parts per billion by volume (ppbV) to interglacial values of ~700 ppbV, and closely resembled patterns of summer insolation in the Northern Hemisphere (Fig. 1), which suggests that insolation variations are an important element of climate cycles controlling atmospheric methane levels (*1, 3*). Recent work on the shallow sections of the GRIP and GISP2 ice cores from central Greenland (*4*), representing the past 40,000 years (*5–7*), further showed that methane concentrations varied rapidly in association with 1000- to 3000-year-long interstadial events inferred from the oxygen isotopic composition of the ice ($\delta^{18}O_{ice}$). Here we present a methane record from the GISP2 ice core for the past 110,000 years (Figs. 1 and 2). Our data verify general patterns exhibited by the Vostok methane record (*1*), verify the GRIP results between 0 and 40,000 years ago (ka) (*5*), document rapid methane variations between 40 and 110 ka, and provide a detailed picture of methane variations and their relation to interstadial events and longer term climate cycles.

We measured the methane concentration of trapped gases in samples from 309 depths in the upper 2810 m of the GISP2 ice core (*8*). Studies of ice structure (*9*), the $\delta^{18}O$ of atmospheric O_2 (*10*), and methane concentrations from the bottom 243 m of the core suggest that the stratigraphy below 2810 m is not continuous (*11*). We report the methane data (Figs. 1 and 2) on a modified GISP2 gas age time scale (*12*), which accounts for the fact that gases are trapped between 80 and 100 m below the surface of the ice sheet and are therefore younger than the surrounding ice. Within the stated uncertainties of this time scale the GISP2 methane record can be directly compared to marine and terrestrial climate records that have been placed on the calendar or SPECMAP (*12*) time scales.

The lifetime of methane in the atmosphere is relatively short, ~9 to 10 years at present (*13, 14*). Before 1800 A.D., the dominant methane source was anaerobic decomposition of organic material in natural wetlands (*15*). Other sources including termites, wild animals, wildfires, methane hydrate release, and the oceans may have accounted for as much as 40% of total methane sources during the preindustrial Holocene and the last glacial maximum (LGM) (*15*). More recently than 1800 A.D., ice core data indicate that anthropogenic emissions significantly affected the methane cycle (*16–18*). The major methane sink is oxidation by tropospheric OH (*19*). Studies of the oxidative capacity of the atmosphere suggest that OH concentrations probably changed on glacial-interglacial time scales primarily in response to changing methane emissions (*20, 21*). These results imply that the ice core methane record before 1800 A.D. primarily reflects changes in rates of emission from the dominant natural source—wetland ecosys-